environmental microbiology

Environmental Microbiology (2015) **17**(6), 1950–1962 doi:10.1111/1462-2920.12468

Involvement of the Acr3 and DctA anti-porters in arsenite oxidation in *Agrobacterium tumefaciens* 5A

Yoon-Suk Kang,[1] Zunji Shi,[1,2] Brian Bothner,[3] Gejiao Wang[2] and Timothy R. McDermott[1]*

[1]*Department of Land Resources and Environmental Sciences,* [3]*Department of Chemistry and Biochemistry, Montana State University, Bozeman, MT 59717, USA.*

[2]*State Key Laboratory of Agricultural Microbiology, College of Life Science and Technology, Huazhong Agricultural University, Wuhan, China.*

Summary

Microbial arsenite (AsIII) oxidation forms a critical piece of the arsenic cycle in nature, though our understanding of how and why microorganisms oxidize AsIII remains rudimentary. Our model organism *Agrobacterium tumefaciens* 5A contains two distinct *ars* operons (*ars1* and *ars2*) that are similar in their coding region content. The *ars1* operon is located nearby the *aio* operon that is essential for AsIII oxidation. The AsIII/H^+ anti-porters encoded by *acr3-1* and *acr3-2* are required for maximal AsIII and antimonite (SbIII) resistance, but *acr3-1* (negatively regulated by ArsR-1) appears more active in this regard and also required for AsIII oxidation and expression of *aioBA*. A malate-phosphate anti-porter DctA is regulated by RpoN and AsIII, and is required for normal growth with malate as a sole carbon source. Qualitatively, a Δ*dctA* mutant was normal for AsIII oxidation and AsIII/SbIII resistance at metalloid concentrations inhibitory to the Δ*acr3-1* mutant; however, *aioBA* induction kinetics was significantly phase-shift delayed. Acr3 involvement in AsIII/SbIII resistance is reasonably well understood, but the role of Acr3 and DctA anti-porters in AsIII oxidation and its regulation is unexpected, and suggests that controlled AsIII trafficking across the cytoplasmic membrane is important to a process understood to occur in the periplasm.

Received 2 October, 2013; accepted 22 March, 2014. *For correspondence. E-mail timmcder@montana.edu; Tel. (+1) 406 994 2190; Fax (+1) 406 994 3933.

Introduction

Arsenic (As) is the most common toxic element in the environment, ranking first on the Environmental Protection Agency Superfund List of Hazardous Substances. From numerous studies conducted in various environments, it is now appreciated that microbial redox transformations are important drivers of As chemical speciation in nature, which in turn dictates As mobility and toxicity (Cullen and Reimer, 1989; Pontius *et al*., 1994; Inskeep *et al*., 2001; Oremland and Stolz, 2003; Stolz *et al*., 2006). As such, in order to more fully understand As behaviour in the environment, it is critical that there be a thorough understanding of microbe–As interactions that underlie arsenite (AsIII) oxidation and arsenate (AsV) reduction.

With regards to the genetic circuitry regulating AsIII oxidation, several important observations have been reported during the past decade. The genes encoding the AsIII oxidase heterodimer, *aioBA*, have been cloned and characterized (vanden Hoven and Santini, 2004; Muller *et al*., 2003), and are phylogenetically distinct from the more recently discovered AsIII oxidase from *Alkalilimnicola ehrlichii* cloned and characterized by Zargar *et al*. (2010; 2012). A two-component signal transduction pair, *aioS* and *aioR*, has been identified (Kashyap *et al*., 2006a; Koechler *et al*., 2010), and the phosphorelay demonstrated to occur between AioS and AioR (Sardiwal *et al*., 2010) is consistent with the two-component signal transduction paradigm (Stock *et al*., 1995). More recently, a periplasmic AsIII binding protein, AioX, has been shown to be essential to AsIII-based signalling and AsIII oxidation (Liu *et al*., 2012). Furthermore, the entire Aio-based signalling process is sensitive to inorganic phosphate and controlled in part by PhoB1 and PhoB2 proteins (Kang *et al*., 2012a) that are the cognate regulatory proteins paired with the phosphate sensing histidine kinase PhoR. We are currently finishing work with PhoR in strain 5A and have found it too is essential for AsIII oxidation and will be reported as a separate study. Another regulatory element controlling *aioBA* expression involves the sigma factor RpoN (Koechler *et al*., 2010; Kang *et al*., 2012b) in conjunction with AioR and is consistent with the *aioBA* promoter region containing a consensus RpoN binding site (Koechler *et al*., 2010; Kang *et al*., 2012b).

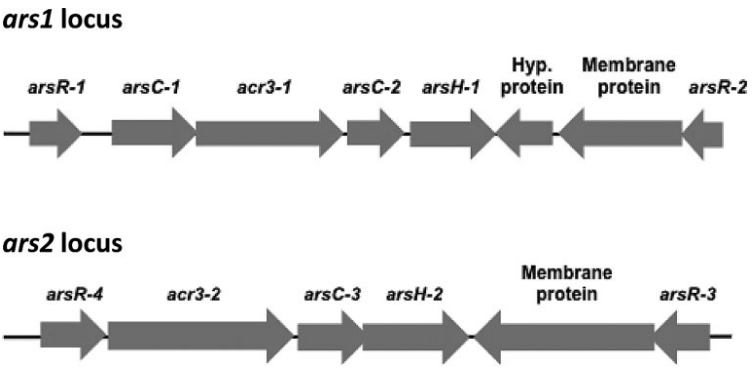

Fig. 1. Gene composition and organization of the *ars1 and ars2* operons in *Agrobacterium tumefaciens* 5A. *arsR* encodes the ArsR repressor, *arsC* codes for arsenate reductase, *arc3* encodes an AsIII/SbIII efflux anti-porter; and *arsH* encodes a H_2O_2-forming NADPH:FMN1 oxidoreductase.

A survey of the *Agrobacterium tumefaciens* strain 5A genome identified RpoN binding sites in the putative promoter regions of several genes not known to be involved in AsIII oxidation (Kang *et al*., 2012b). Expression analysis of several of these genes showed that a *dctA* homologue was upregulated in cells exposed to AsIII (Kang *et al*., 2012b). This DctA is similar to rat and plant mitochondrial C4-dicarboxylate transporters that facilitate the exchange of malate and phosphate (Kaplan and Pedersen, 1985; Furbank *et al*., 1990) but that will readily replace phosphate with AsV in the exchange reaction (Furbank *et al*., 1990). In the context of As trafficking, we previously found that a Na^+/H^+ anti-porter was also required for AsIII oxidation, though it did not have an apparent regulatory role with respect to the expression of *aioSR* or *aioBA* as monitored with reverse transcriptase polymerase chain reaction (PCR) (Kashyap *et al*., 2006b).

The apparent roles of proteins involved in membrane As trafficking prompted us to take a closer look at this particular issue, examining the relative importance of DctA and the two different Acr3 anti-porters encoded by *acr3* genes in two disparately located *ars* operons in strain 5A. Herein, we summarize the results of studies that suggest that As trafficking in and out of the cell is somehow linked to the normal expression of *aioBA* genes and for AsIII oxidation, a process viewed to occur in the periplasm.

Results

Identification and genetic organization of ars *genes in* A. tumefaciens *5A*

Our interests in the *A. tumefaciens* 5A *ars* genes in part stemmed from our recent discovery that the ArsR1 repressor is involved in the regulation of genes located near the *aio* locus (Kang *et al*., 2012a). Additionally, the *A. tumefaciens* 5A genome contains two *ars* loci, referred to here as *ars1* and *ars2* (Fig. 1), and thus it was also of interest to begin examining their relative roles in arsenic metabolism in this organism. The *ars1* and *ars2* loci are similar in terms of being bracketed by divergently oriented *arsR* genes highly conserved among many arsenic-resistant bacteria (Silver *et al*., 1993; 2001; Diorio *et al*., 1995; Sato and Kobayashi, 1998; Butcher *et al*., 2000). The two *ars* loci are also very similar with regards to annotated genes and their orientation except that the *ars1* locus contains an additional *arsC* and an open reading frame annotated as a hypothetical protein (Fig. 1).

Analysis of the *ars* loci began by creating a *tetRA* cassette insertion mutation in *arsR*-1 to determine whether it or any downstream genes in the apparent operon might be involved in AsIII oxidation or resistance. Qualitative analysis of AsIII oxidation via silver nitrate staining revealed a negative AsIII oxidation phenotype for the *arsR1*::*tetRA* mutant (Fig. 2). Reverse transcription polymerase chain reaction (RT-PCR) was then used to illustrate the polar effects of the *arsR1*::*tetRA* insertion on downstream genes expression (e.g. see Supporting Information Fig. S1). Further, the expected role of ArsR-1 as a repressor was confirmed by conducting ArsR-1 binding

Fig. 2. Qualitative analysis of AsIII oxidation using $AgNO_3$ staining. $MMNH_4$ agar plates containing 50 μM Pi with 0.5 mM AsIII were used for the assays. After streak inoculation and 48 h incubation, plates were flooded with a 0.1 M $AgNO_3$ solution. Brown precipitate indicates the presence of arsenate, whereas yellow indicates arsenite. Note that robust growth occurred in all streak quadrants.

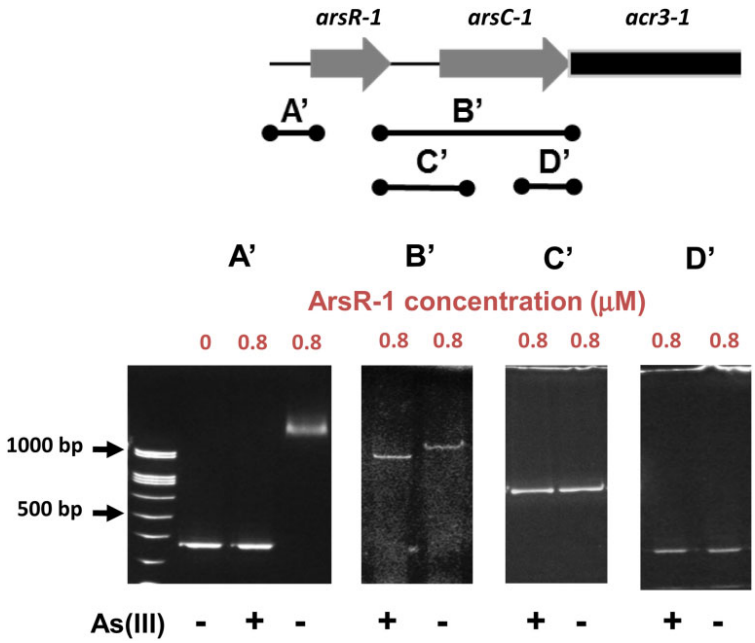

Fig. 3. EMSA analysis of ArsR-1 interaction with four different regions of the *ars1* operon locus. A′: 321 bp, *arsR-1* upstream region; B′: 1184 bp, 3′ terminus of a*rsR-1* to 5′ terminus of *acr3-1*; C′: 585 bp, 3′ region of *arsR-1* to 5′ region of *arsC-1*, D′: 343 bp, 3′ prime region of *arsC-1* to 5′ terminus of *acr3-1*. Each PCR fragment was incubated with purified His_6-ArsR-1 in the absence or presence of 1 mM AsIII (as indicated). Samples were electrophoresed in non-denaturing 6% polyacrylamide gels and stained with ethidium bromide. The shifted bands indicate DNA-ArsR-1 complexes. Each lane contains 35 nmol of DNA and 0 or 0.8 μM of His_6-ArsR-1.

assays using His-tagged purified ArsR-1 along with four DNA probes generated by PCR. In the absence of AsIII, an ArsR-1 binding site (and thus a putative ArsR-1 sensitive promoter) was found upstream of *arsR-1* (referred to as operon region A′ in Fig. 3) and within the *arsC-1* coding region (region B′ in Fig. 3), but not in the region between *arsR-1* and *arsC-1* (region C′ in Fig. 3), nor immediately upstream of *acr3-1* (region D′ in Fig. 3). Taken together, the RT-PCR and electrophoretic mobility shift assay (EMSA) showed that the ArsR-1 is auto-regulated, regulates the expression of downstream genes in an AsIII-dependent manner, and that its DNA-binding behaviour is entirely consistent with its characterization as an AsIII sensitive repressor (Silver *et al*., 1993; 2001; Diorio *et al*., 1995; Sato and Kobayashi, 1998; Butcher *et al*., 2000).

We next sought to identify the gene(s) involved in the negative AsIII oxidation phenotype in the *ars1* locus. Since *arsC* genes code for arsenate (AsV) reductases, we reasoned that the inactivation of *arsC-1* and or *arsC-2* would not influence cellular AsIII oxidation except to perhaps strengthen it by decreasing background AsV reduction activity. Therefore, non-polar deletion mutations were individually introduced into *arsR-1*, *acr3-1* and *arsH-1*. The Δ*arsR-1* mutant was positive for AsIII oxidation (Fig. 2), as was the Δ*arsH-1* mutants (results not shown); however, the Δ*acr3-1* mutant was negative for this trait (Fig. 2). Reintroducing the wild-type *acr3-1* gene and additional upstream sequence located in *arsC-1* (including the region within the *arsC-1* coding region implied to contain a putative promoter as inferred by an ArsR-1 binding site, see Fig. 3) complemented the Δ*acr3-1* back to wild-type status with respect to AsIII oxidation (Fig. 2). This confirmed the functional importance of *acr3-1* to AsIII oxidation. Introducing a deletion into the *acr3-2* coding region did not affect AsIII oxidation as assayed via silver nitrate staining on $MNNH_4$ agar containing 1.0 mM, 2.0 mM or 3.0 mM AsIII (Supporting Information Fig. S2).

The operon nature of the *ars1* locus was also clearly shown by the results of RT-PCR experiments (Supporting Information Fig. S3). RT-PCRs were conducted with primers specific to within the coding regions of the *ars1* genes so as to determine whether they share the same transcript (see Supporting Information Fig. S3 caption). In each case, the RT-PCRs generated amplicons that spanned from: (i) within the 3′ coding region of *arsR-1* to within the 5′ coding region of *arsC-1*; (ii) within the 3′ coding region of *arsR-1* to within the 5′ coding region of *acr3-1*; (iii) within the 3′ coding region of *arsC-1* to the within the 5′ coding region of *acr3-1*; and (iv) within the 3′ coding region of *arsC-2* to within the 5′ coding region of *arsH* (Supporting Information Fig. S3). In each case, relative expression levels were either undetectable or lower in cells not exposed to AsIII but elevated in AsIII-exposed cells. Also, and as expected, in each case elevated constitutive expression (i.e. lack of AsIII control) of genes downstream from *arsR-1* was observed in the Δ*arsR-1* mutant (Supporting Information Fig. S3) and again is evidence that these genes are controlled to some degree by ArsR-1. We also draw attention to the observation that while the RT-PCRs depicted in Supporting Information Fig. S3 are qualitative with respect to apparent transcript abundance in the RT reactions, there appears to be other regulatory controls originating from within the *arsC-1* coding region as evidenced by differences in relative strengths of downstream amplicons in the absence of

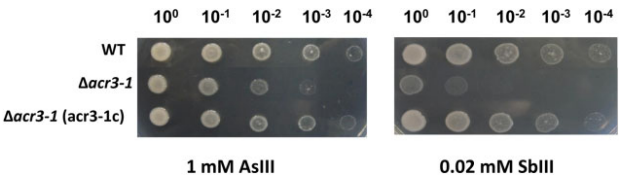

Fig. 4. Acr3-1 is involved in trivalent metalloid resistance. Growth of the wild-type, Δ*acr3-1*, and *acr3-1* complemented strain harbouring pJQ200SK-*acr3c* on MMN agar medium containing 1.0 mM AsIII or 20 mM SbIII. Each culture was first normalized to O.D. ~ 0.4, and then serially diluted 10-fold, with each dilution spotted onto the agar medium (10 ml each) and incubated at 30°C for 24 h.

AsIII (Supporting Information Fig. S3). This interpretation is also consistent with our ability to rescue the Δ*acr3-1* mutant with a DNA fragment that included upstream *arsC-1* coding region that was also found to contain an ArsR-1 binding site (Fig. 3, discussed above).

AsIII and SbIII sensitivity

Additional testing then examined the deletion mutants for metalloid sensitivity. Growth of the Δ*arsR-1* and Δ*arsH-1* mutants on $MMNH_4$ agar containing 1.0 mM AsIII or 20 μM SbIII was equivalent to wild type with respect to sensitivity (results not shown), whereas the Δ*acr3-1* mutant was more sensitive (Fig. 4). Metalloid resistance of the Δ*acr3-2* mutant (though still Acr3-1$^+$) was equivalent to the wild-type parental strain on $MMNH_4$ agar containing 1.0–2.0 mM AsIII or 20 –40 μM SbIII (data not shown) but exhibited sensitivity to 3.0 mM AsIII and 60 μM SbIII (Supporting Information Fig. S4).

The different AsIII oxidation and AsIII/SbIII resistance phenotypes of the Δ*acr3-1* and Δ*acr3-2* mutants suggested Acr3-1 and Acr3-2 may be structurally different. Their inferred amino acid sequences are 88.3% identical/94% similar, and as would be predicted, they are very closely related phylogenetically (Supporting Information Fig. S5A). Both of the 5A Acr3 proteins belong to cluster II Acr3s first described by Achour and colleagues (2007), with Acr3-2 apparently modified from Acr3-1 by losing two and adding one predicted protein binding sites (Supporting Information Fig. S5B). Several protein structure prediction programs predict the N-terminal and C-terminal domains for both Acr3-1 and Acr3-2 are located in the cytoplasm and share the same number of transmembrane spanning regions, though differing in terms of sizes (Supporting Information Fig. S5B). In summary, while Acr3-1 and Acr3-2 differ structurally and functionally, the phylogenetic and primary protein structural analyses imply that Acr3-1 and Acr3-2 are AsIII efflux anti-porters involved in AsIII trafficking and arsenic resistance.

To understand the basis for the defective AsIII oxidation in the Δ*acr3-1* mutant, we examined the expression of AsIII oxidase structural genes (monitored as an *aioB*::*lacZ* reporter) in the wild-type strain, and in the Δ*acr3-1* and Δ*acr3-2* mutants. Growth of the wild-type and Δ*acr3-2* mutant strains in liquid media was not affected by 0.5 or 1.0 mM AsIII, whereas the Δ*acr3-1* mutant exhibited significant sensitivity to AsIII (Fig. 5A); growth declined soon after raising the AsIII concentration in the growing culture to 1.0 mM (Fig. 5A) and thus was similar to that observed in the agar sensitivity assays (Fig. 4). We note also that the decline in culture optical density was accompanied by a commensurate decrease in viable cell plate counts (results not shown). Induction of *aioB*::*lacZ* in the Δ*acr3-1* mutant followed a similar profile as in the wild-type strain

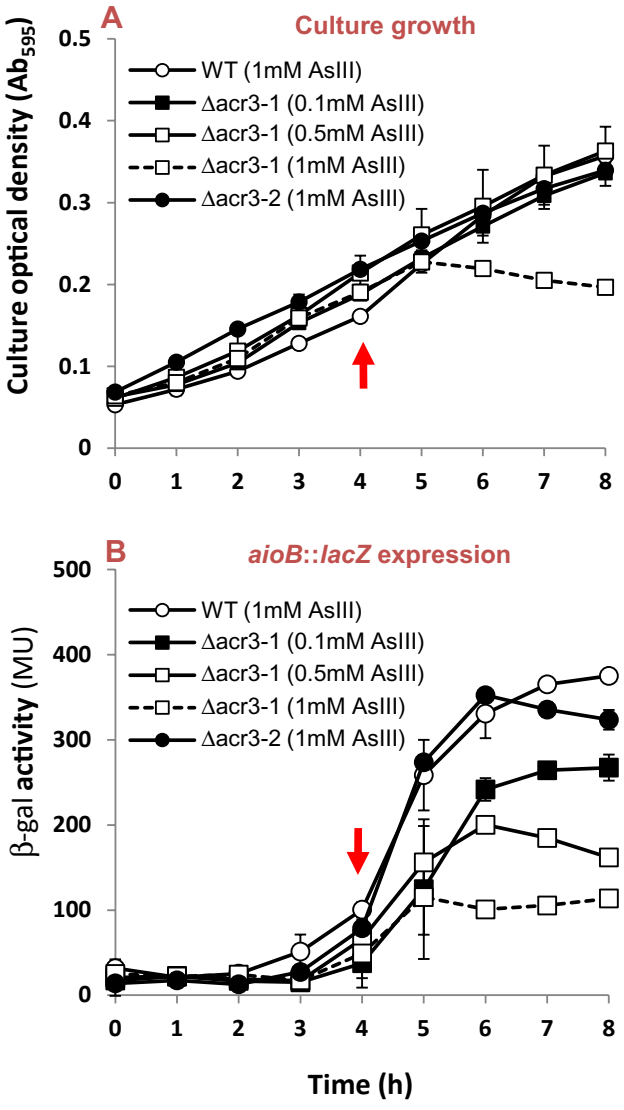

Fig. 5. Characterization of the Δ*acr3-1* and Δ*acr3-2* mutants for growth (A) and regulation of *aioB* (B). For each culture, cells were inoculated into $MMNH_4$ media containing 50 mM phosphate and 100 mM AsIII, incubated for 4 h, at which time additional AsIII was added (arrow). Where visible, the error bars represent ± 1 SD.

with no AsIII addition beyond the 0.1 mM used to induce *aioB*::*lacZ*. However, within 1 h of AsIII addition to the Δ*acr3-1* mutant, *aioB*::*lacZ* expression appeared to slow at 0.5 mM AsIII, or cease completely at 1.0 mM (Fig. 5B). The decline in Δ*acr3-1* mutant reporter enzyme content in the 0.5 mM AsIII treatment is perhaps attributable to variably reduced *aioB*::*lacZ* expression relative to cell growth, resulting in moderate dilution of cellular β-galactosidase levels as viewed at the whole culture level.

Growth responses and *aioB*::*lacZ* reporter induction kinetics in the Δ*acr3-2* mutant were very similar to the wild-type strain regardless of AsIII concentration (Fig. 5, Supporting Information Fig. S6). At AsIII levels ≤ 1.0 mM, both strains continued to grow (Fig. 5A) and to synthesize β-galatocsidase in a similar fashion (Fig. 5B). However, when AsIII levels were spiked to 3 mM (upper sensitivity for the Δ*acr3-2* mutant, Supporting Information Fig. S4) midway during *aioB*::*lacZ* induction, cell growth and synthesis of the reporter enzyme ceased immediately in all strains (Supporting Information Fig. S6).

Involvement of DctA in regulating aioBA

In a recent study examining the role of the sigma factor RpoN in regulating AsIII responsive genes in *A. tumefaciens* strain 5A, we found a *dctA* homologue coding region that is preceded by a consensus RpoN binding site and that was upregulated by AsIII (Kang *et al.*, 2012b). This particular DctA shares homology with plant malate–phosphate anti-porters (Kaplan and Pedersen, 1985; Furbank *et al.*, 1990) that will replace phosphate with arsenate in the anti-port process (Furbank *et al.*, 1990). To examine this anti-porter further, we created a deletion mutation in the *dctA* coding region and then assessed its potential role in malate acquisition, AsIII sensitivity, and in AsIII oxidation. Growth of the Δ*dctA* mutant was impaired in liquid $MMNH_4$ medium in which mannitol was replaced by malate as the sole carbon source (Fig. 6A), and thus illustrating evidence that this particular DctA is indeed involved with malate acquisition. Growth of the Δ*dctA* mutant was not impaired at 1.0 mM AsIII, and likewise growth was not influenced when the Δ*dctA* was introduced into the Δ*acr3-1* mutant (Fig. 6B). Surprisingly, upregulation of the (*aioB*::*lacZ* reporter was phase shift delayed by approximately 3 h and reduced by roughly half relative to the wild-type strain (Fig. 6C). Additional induction experiments found the Δ*dctA* mutant was similar to the wild-type and the Δ*acr3-2* mutant strain in its sensitivity to 3 mM AsIII (Supporting Information Fig. S6).

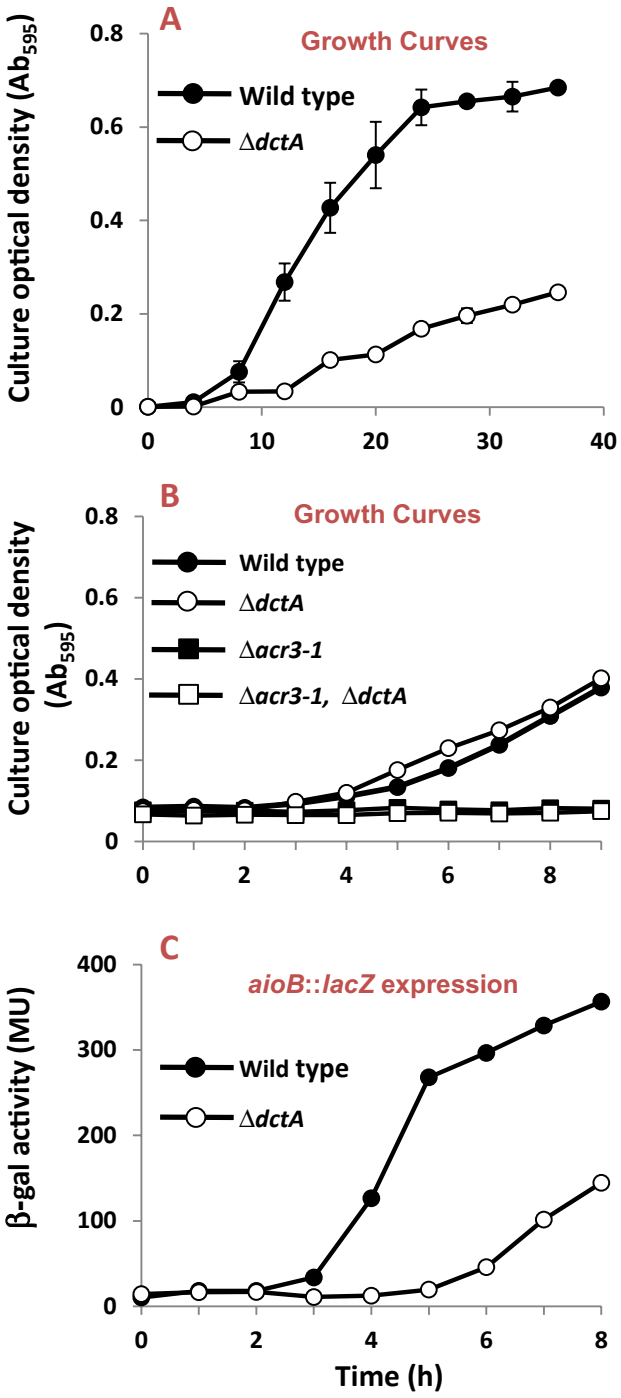

Fig. 6. Characterization of the Δ*dctA* mutant.
A. Growth in $MMNH_4$ media where the mannitol was replaced by malate.
B. Growth in $MMNH_4$ media containing 1.0 mM AsIII.
C. *aioB:: lacZ* reporter gene expression in the wild-type and the Δ*dctA* mutant in $MMNH_4$ media containing 50 mM phosphate and 100 mM AsIII. Results shown are for duplicate cultures for each treatment. Where visible, the error bars represent ± 1 SD.

Discussion

The literature is replete with documentation of *ars* operons in *Bacteria* and related systems in *Archaea* and

yeast, and the role these genes play in coding for resistance to arsenic and antimony (e.g. see reviews by Rosen, 1999; Mukhopadhayay *et al*., 2002; Rosen, 2002). Reports of multiple *ars* operons in chromosomes are less frequent though, thus far being limited to the phyla *Actinobacteria* (*Corynebacterium glutamicum*, Ordóñez *et al*., 2005), α-*Proteobacteria* (*Ochrobactrum tritici*, Branco *et al*., 2008), *Betaproteobacteria* (*Herminiimonas arsenicoxydans*, Muller *et al*., 2003; *Thiomonas* sp. 3As, Arsène-Ploetze *et al*., 2010) *Nitrospirae* (*Leptospirillum ferriphilum*, Li *et al*., 2010) and the *Firmicutes* (*Geobacillus kaustophilus*, Cuebas *et al*., 2011). Finding multiple *ars* operons in *A. tumefaciens* 5A documents an additional alphaproteobacterium.

At the minimum, *ars* operons contain an *arsR*, *arsC* and an *arsB* as found in *Staphylococcus* plasmid pI258 (Ji and Silver, 1992a,b; Rosenstein *et al*., 1992). Alternatively, *ars* operon composition can also include *arsD* and *arsA* as has been documented for *Escherichia coli* (Rosen *et al*., 1992), or *arsH* and *acr*3. ArsD exhibits weak repressor activity, but its primary function is currently viewed to be an arsenic metallochaperone (Wu and Rosen, 1993; Chen and Rosen, 1997; Lin *et al*., 2006; Ajees *et al*., 2011). The *arsC* gene encodes a small cytoplasmic AsV reductase that is required for optimum As resistance. ArsH is a flavoprotein (Ye *et al*., 2007) that also participates in arsenic resistance in *Serratia marcesens* and *Sinorhizobium meliloti* (Ryan and Colleran, 2002; Yang *et al*., 2005), but apparently not in *Acidothiobacillus ferrooxidans* or *Synechocystis* (Butcher *et al*., 2000; Lopez-Maury *et al*., 2003). ArsB is an AsIII efflux pump that can convert from using adenosine triphosphate (ATP) hydrolysis as an energy source to using membrane potential (Tisa and Rosen, 1989; Dey *et al*., 1994; Dey and Rosen, 1995). The ability of ArsB to use ATP derives from its association with ArsA, an ATPase (Chen *et al*., 1986). Gene duplication within these operons is also not unusual, as was found in *A. tumefaciens* 5A (Fig. 1).

As thus far described in the literature, regulation of *ars* operons is invariably via an ArsR repressor protein, usually encoded by an *arsR* contained in the same operon it controls (i.e. autoregulatory) or positioned close nearby. This was also the case with ArsR-1 controlling the *ars1* operon in *A. tumefaciens* 5A (Fig. 3, Supporting Information Fig. S3) in a fashion totally consistent with the well-known function of ArsR repressors that block transcription. When AsIII enters the cell via an aquaglyceroporin such as GlpF (Rosen, 1999; 2002; Mukhopadhayay *et al*., 2002), it binds to the ArsR homodimer, bringing about a conformational change causing ArsR to release from the DNA that then is opened up to transcription. Showing that ArsR1 acts as a repressor of the *ars1* operon (Fig. 3, Supporting Information Fig. S1 and S3) serves to authenticate it as a canonical *ars* repressor in addition to functioning in the same capacity to co-regulate the expression of the nearby *pstS1* and *phoB1* genes that are located immediately adjacent to the *aioXSRBA* genes that are essential for AsIII oxidation (Kang *et al*., 2012a). Thus, this study illustrates a scenario similar to that described by Murphy and Saltikov (2009), where the ArsR2 protein in *Shewanella* sp. strain ANA-3 controls the expression of *arrAB* (arsenate respiration) as well as *arsC* (arsenic detoxification).

In addition, the current study also illustrates the ArsR-1 protein binding at more than one location within the *ars1* operon, in this instance binding upstream of *arsR-1* as well as within the *arsC-1* coding region. In both cases, binding was AsIII-dependent (Fig. 3) and thus as such is completely consistent with the known manner in which ArsR repressors behave (San Francisco *et al*., 1990; Wu and Rosen, 1993). The presence of a promoter in the *arsC-1* coding region can be inferred from three independent observations. First, the *arsC-1* coding region contains an ArsR-1 binding site (Fig. 3), implying the presence of an associated promoter. Second, expression of genes downstream of *arsC-1* appear to be regulated differently from that observed for *arsR-1* and *arsC-1* (Supporting Information Fig. S3). Specifically, while *arsR-1* and *arsC-1* require AsIII for induction and are under the control of ArsR-1 (Supporting Information Fig. S1 and S3), *acr3-1*, *arsC-2* and *arsH* are expressed in the absence of AsIII (Supporting Information Fig. S3), though are nevertheless upregulated by AsIII in an ArsR-1 dependent manner, and their constitutive expression is enhanced in the Δ*arsR-1* mutant (Supporting Information Fig. S3). And finally third, subcloned DNA in pJQ200SK containing the *acr3-1* coding region along with DNA that includes the ArsR-1 binding region in *arsC-1* allowed for complementation of the Δ*acr3-1* mutant (Fig. 2). We have shown previously that the *lac* promoter adjacent to the multicloning cite in the complementation vector pJQ200SK is not sufficient to initiate expression of cloned DNA in strain 5A nor is it sensitive to AsIII (Liu *et al*., 2012). Therefore, there must be a promoter upstream of *acr3-1* and included in the complementing DNA.

While the above observations concerning an *arsC-1* proximal promoter are consistent with each other, they nevertheless present a conundrum with respect to reconciling those observations with the differing AsIII oxidation phenotypes of the *arsR-1*::*tetRA* and Δ*arsR-1* mutants (Fig. 2). The following observations are consistent with the conclusion that regulatory control of *acr3-1* derives from the *arsR-1* proximal promoter: i) *arsR-1*, *arsC-1* and *acr3-1* (as well as *arsC-2* and *arsH*) are transcriptionally linked (Supporting Information Fig. S3); ii) the polar effect of the *tetRA* insertion in *arsR-1* disrupts expression of downstream genes (Supporting Information Fig. S1); iii) the polar effect of the *tetRA* insertion in *arsR-1* resulted in

a negative AsIII oxidation phenotype of the *arsR-1*::*tetRA* mutant (Fig. 2); and iv) predictably, the Δ*arsR-1* mutation leads to constitutive expression of all genes in this operon (Supporting Information Fig. S3) and is positive for AsIII oxidation (Fig. 2). However and nevertheless, equally clear is the AsIII-independent expression of *acr3-1* (Supporting Information Fig. S3), presumably driving from a promoter within the *arsC-1* coding region that corresponds to the ArsR-1 binding site (Fig. 3). The latter suggests that regulation stemming from the *arsR-1* promoter would be unnecessary, which is inconsistent with the negative AsIII oxidation phenotype of the *arsR-1*::*tetRA* mutant (Fig. 2). All of these observations are reproducible, though at present are difficult to completely square with one another but will be the target of additional future efforts aimed at sorting through possible explanations.

Acr3 anti-porters are also often found in *ars* operons and were first characterized in yeast (Wysocki *et al*., 1997). They have predicted or confirmed transmembrane topology (Wysocki *et al*., 1997; Sato and Kobayashi, 1998; Ghosh *et al*., 1999; Aaltonen and Silow, 2008; Fu *et al*., 2009; Indriolo *et al*., 2010) and display an AsIII/H^+ and SbIII/H^+ anti-porter mechanism (Maciaszczyk-Dziubinska *et al*., 2010). Acr3 anti-porters also occur in many different bacteria (Cai *et al*., 2009), conferring AsIII and AsV resistance (Wysocki *et al*., 1997; Sato and Kobayashi, 1998; Xia *et al*., 2008; Fu *et al*., 2009). Further, in protein searches we found several methanogen accessions in the NCBI database that exhibit promising homology with Acr3 (examples: YP_005380238, *Methanocella conradii*, e-value = 2e-46, 33% identity/55% similarity; *Methylosarcina fibrata* WP_020562285, e-value = 2e-46, 32% identity/53% similarity; *Methanocella arvoryzae* YP_686206, e-value = 2e-46, 33% identity/55% similarity). These archaeal Acr3 proteins exhibit much higher identity (e.g. 90%) with those found in the *Firmicutes*.

We are aware of but two reports of Acr3 mediating tolerance to both AsIII and SbIII in a bacterium (Lopez-Maury *et al*., 2003; Branco *et al*., 2008). Duplication of *arsB* and *acr3* genes enhances cellular resistance to arsenic and antimony (Ordóñez *et al*., 2005) but with differential capacity (Ordóñez *et al*., 2005; Branco *et al*., 2008) as was shown with the Acr3-1 and Acr3-2 in *A. tumefaciens* strain 5A. Acr3-1 provides maximal resistance up to roughly 1.0 mM AsIII and 20 μM SbIII, beyond which Acr3-2 assists (Fig. 4, Supporting Information Fig. S3). Consequently, the study summarized herein broadens the documentation in this regard. That Acr3-1 and Acr3-2 in strain 5A differ in their apparent capacity to provide resistance to AsIII or SbIII (Fig. 4, Supporting Information Fig. S3) and presumably derives from relative differences in the anti-port efficiency with these metalloids. As suggested by their phylogenetic relatedness (Supporting Information Fig. S4A), these anti-porters are quite similar with respect to number, position and length of the membrane spanning regions (Supporting Information Fig. S4B), though they differ in the position of predicted protein binding sites, suggesting potential targets for future efforts aimed at characterizing the AsIII/SbIII trafficking mechanisms of these anti-porters.

The discovery that AsIII oxidation and or *aioB* expression is influenced in the Δ*acr3* and Δ*dctA* mutants was unanticipated. Since all mutants were generated by non-polar deletions, expression of downstream genes would not be affected. The involvement of transporters in AsIII oxidation is not without precedent as we have previously shown that a Mrp-type Na^+/H^+ anti-porter is required for AsIII oxidation (Kashyap *et al*., 2006b), and thus strongly arguing that the Acr3, DctA and the Mrp Na^+/H^+ anti-porters share a common theme that involves arsenic trafficking in some fashion. The Acr3 anti-porter is well established as an important mechanism for exporting AsIII (discussed above), and the type of DctA involved in this instance is a homologue to a malate–phosphate anti-porter (Kaplan and Pedersen, 1985; Furbank *et al*., 1990) shown to substitute AsV for phosphate in the anti-port process (Furbank *et al*., 1990). To our knowledge, its potential for transporting AsIII has not been investigated, but given that *dctA* expression is induced by AsIII and apparently requires RpoN (Kang *et al*., 2012b), its functional link with AsIII oxidation (Fig. 6) should not be viewed as a coincidence.

Growth characteristics in response to AsIII cannot be directly compared between surface growth on solid agar medium and liquid media. In the former, AsIII exposure is diffusion limited and AsIII oxidation can reduce overall toxicity of the immediate cell environment, whereas in liquid media with constant mixing there is no diffusion limitation. Consequently, the wild type, Δ*acr3-2* and Δ*dctA* strains were all capable of robust growth and AsIII oxidation on 3 mM $MMNH_4$ agar (Supporting Information Fig. S2) but exhibited immediate cessation of both growth and *aioB*::*lacZ* expression with a sudden spike of 3 mM AsIII that apparently at least temporarily overwhelms all of the cellular capacity to efflux AsIII (Supporting Information Fig. S6). This is contrast to the mixed properties of the Δ*acr3-1* mutant. It could grow on $MMNH_4$ agar or in $MMNH_4$ liquid media containing 0.5 mM AsIII (Fig. 2, Fig. 5A) or 1.0 mM AsIII agar (Fig. 4), though not in liquid $MMNH_4$ media spiked with 1.0 mM AsIII (Fig. 5A). Unlike the wild type or other mutants examined in this study which displayed AsIII oxidation at the highest AsIII levels (Supporting Information Fig. S2), this activity in the Δ*acr3-1* mutant was restricted and uncoupled from growth.

Our future work will be taking a closer look at all three anti-porters to more clearly establish their relative roles in

shuttling arsenic across the cytoplasmic membrane and to better understand the consequences when they are not functioning. While AsIII flow direction for the Mrp Na^+/H^+ and DctA anti-porters has yet to be characterized in a Gram-negative bacterium, the literature is clear in terms of how Acr3 anti-porters export AsIII from the cytoplasm and are critical to AsIII resistance (Rosen, 1999; 2002; Mukhopadhayay *et al*., 2002). As would be predicted then, this is also the case for *A. tumefaciens* 5A, where AsIII concentrations in the range of 1.0 mM proved lethal (Fig. 5A) when the Acr3-1 anti-porter was not functioning.

At present, the apparent requirement of AsIII export from the cytoplasm being required for AsIII oxidation is somewhat of a paradox. The evidence to date presents a strong argument that AsIII detection and initial steps of signal transduction (Kashyap *et al*., 2006a; Koechler *et al*., 2010; Sardiwal *et al*., 2010; Liu *et al*., 2012), as well as AsIII oxidation itself (Anderson *et al*., 1992; Santini *et al*., 2000; Lebrun *et al*., 2003; vanden Hoven and Santini, 2004; Duquesne *et al*., 2008; Prasad *et al*., 2009; Lieutaud *et al*., 2010), all occur in the periplasm. Presumably, accumulation of AsIII in the cytoplasm may create conditions whereby proteins critical to several cellular activities are inactivated, partially or in total, and potentially accounting for the decreased *aioB* expression (Fig. 5B, Fig. 6C). However, the Δ*acr3-1* mutant exhibited robust, apparently uninhibited growth in $MMNH_4$ liquid (Fig. 5A) or on agar (Fig. 2) media containing 0.5 mM AsIII, yet is inactive for AsIII oxidation (Fig. 2). Based on the observations made in this study, it would seem that either AsIII accumulation very selectively inactivates specific proteins essential to some aspect of *aio* expression while not significantly influencing growth-essential proteins (e.g. Fig. 5B), and or the AsIII oxidation process is compartmentalized in unanticipated ways. Clearly, controlled AsIII trafficking across the cytoplasmic membrane is important to a process viewed to occur in the periplasm.

Materials and methods

Bacterial strains and growth conditions

The bacterial strains, plasmids and primer sequences used in this study are listed and briefly described in Table 1. The *A. tumefaciens* strains were cultured at 30°C in a defined minimal mannitol medium ($MMNH_4$) (Somerville and Kahn, 1983) containing mannitol as a carbon and energy source with aeration by shaking. *Escherichia coli* strains Top10 and S17-1 were grown at 37°C in Luria–Bertani (LB) medium. Bacterial growth was monitored via measurements of culture optical density using a SpectraMax microtiter plate reader (Molecular Devices, California). Plasmid isolation, gel electrophoresis, transformation and PCR amplification of DNA were conducted as described previously (Kang and Park, 2010; Kang *et al*., 2012a). When required, the mannitol in $MMNH_4$ medium was replaced with malate, or the $MMNH_4$ medium was supplemented with 100 μg ml^{-1} kanamycin (Km) for pLSP selection and maintenance, 80 μg ml^{-1} gentamycin (Gen), 20 μg ml^{-1} tetracycline (Tc) or 15% sucrose for the pJQ200SK selection. Depending on the application, *E. coli* was grown with 50 μg ml^{-1} Km, 20 μg ml^{-1} Gen, 20 μg ml^{-1} Tc.

Construction of A. tumefaciens *5A mutant strains*

The Δ*arsR-1* deletion mutant was constructed by first PCR amplifying the N-terminal region of *arsR-1* from the strain 5A chromosome spanning from 166 bp upstream of the *arsR-1* start codon into the *arsR-1* coding region (primers arsR-1f/1r, Table 1), resulting in a 321 bp amplicon. The 3′ region of *arsR-1* plus 264 bp downstream DNA was amplified (primers arsR-2f/2r, Table 1) resulting in an amplification product of 327 bp. The first fragment was ligated into pCR2.1-TOPO using the restriction enzyme *BamH*I and *EcoR*I, and then the second fragment was also ligated into pCR2.1-TOPO plasmid harbouring the first *arsR-1* fragment by the treatment with *EcoR*I and *Xba*I. The total 648 bp fragment was then subcloned into *BamH*I x *Xba*I-digested pJQ200sk, giving pJQ200sk–*arsR-1*. This plasmid was transformed into *E. coli* S17-1 and then mobilized to *A. tumefaciens* 5A by biparental conjugation. Selection of the Δ*arsR-1* deletion mutant was performed by two-step selection, wherein the initial single recombinants were selected on $MMNH_4$-Gen and then on $MMNH_4$ agar with 15% sucrose, which selects for loss of pJQ200SK (levansucrase-based selection against *sacB*), indicating a double recombinant. The *arsR-1* deletion mutation was confirmed by PCR. Construction of the Δ*acr3-1*, Δ*acr3-2* and Δ*arsH-1*, and Δ*dctA* mutants used cross-over PCR as we have previously described (Kang and Park, 2010; Kang *et al*., 2012a) using primers described in Table 1.

Trivalent metalloid survival and sensitivity assays

For AsIII survival experiments, exponential cultures were inoculated into 20 ml of $MMNH_4$ liquid medium at 30°C with agitation and then at specified times, AsIII (0.1, 0.5 and 1 mM) was added with continued monitoring of culture optical density. During this incubation period, cells were harvested at 1 h intervals and washed with fresh $MMNH_4$ medium (minus mineral and trace elements), serially diluted, plated on a LB agar plates, incubated at 30°C for 24 h and then colonies counted.

AsIII sensitivity assays were performed by two different procedures. Wild-type and mutant cells were streaked on $MMNH_4$ plate containing 0.1 mM antimonite (SbIII) (added as potassium antimonyl tartrate) or 1 mM AsIII and then

Table 1. Bacterial strains, plasmids and primers used in this study.

Strain or plasmid	Relevant markers and characteristics	Reference or source
Strains:		
Agrobacterium tumefaciens		
5A	Wild type, soil isolate, As(III) oxidizing	Lab stock
arsR1::tetRA	TetR, *arsR1* mutant by *tetRA* genes interruption	Lab stock
Δ*arsR1*	*arsR1* gene deletion mutant	This study
Δ*acr3-1*	*acr3* gene deletion mutant	This study
Δ*acr3-2*	*acr3-2* gene deletion mutant	This study
Δ*arsH1*	*arsH1* gene deletion mutant	This study
5A (P*aioB*)	KmR, 5A with pLSP-P*aioB*	Lab stock
Δ*acr3* (P*aioB*)	KmR, Δacr3 with pLSP-P*aioB*	This study
Δ*acr3* (pJQ200sk-acr3c)	GenR, acr3 gene complemental strain	This study
Escherichia coli		
S17-1	Pro-Mob+; conjugation donor	Lab stock
Top10	High-competency cloning host	Invitrogen
HB101	F- recA13 pro Smr	Boyer and Roulland-Dussoix, 1969
Plasmid:		
pCR2.1-TOPO	PCR TA cloning vector	Invitrogen
pRK2013	RK2 derivative Kmr Mob+ Tra+ ColE1	Ditta *et al*., 1980
pJQ200sk	GenR, *traJ*, *oriT*, *sacB*, suicide vector	Lab stock
pJQ200sk-arsR1	pJQ200sk with *arsR1*-deleted region	This study
pJQ200sk-acr3	pJQ200sk with *acr3*-deleted region	This study
pJQ200sk-acr3-2	pJQ200sk with *acr3-2*-deleted region	This study
pJQ200sk-arsH1	pJQ200sk with *arsH1*-deleted region	This study
pJQ200sk-acr3c	pJQ200sk containing *acr3* complete gene	This study
pLSP-PaioB	pLSP-KT2lacZ with *aioB* promoter region	Lab stock
Primers:		
P4/P5	GACGTTGCCTATCCCGATGAAGAT / GTTTGTTGATTGGCCAGGTGTAGG	For RT-PCR of *aioB-aioA* (Kashyap *et al*., 2006a,b)
arsR-1f/1r (321 bp)	CGCGGATCCCGCGGTACGGAAGGTGATT / CGCGAATTCTGCGCCGACATGGTATTTTG	For deletion of *arsR1* gene & for ArsR1-ParsR1 binding assay
arsR-2f/2r (327 bp)	CGCGAATTCGCTCCACTCATTGCCGAACTTACG / CGCTCTAGAGCTCAACATGGCCACAACTGC	
acr3-1f/1r (230 bp)	CGCGGATCCCGATCGCCTGGCCCTTGAAACA / CCCATCCACTAAACTTAAACACAGATGAGGATGGCGACAGGAAT	For deletion of *acr3* gene
acr3-2f/2r (295 bp)	TGTTTAAGTTTAGTGGATGGGTGCCGCGATCAGTCTCTTC / CGCTCTAGAGCGGCTGGGCGGGGTTTTC	
acr32-1f/1r (439 bp)	CGCGGATCCAAACTTTTCGGCTTCTGG / CCCATCCACTAAACTTAAACAGATTGCGACCGGGATATTCACCTT	For deletion of *acr3-2* gene
acr32-2f/2r (287 bp)	TGTTTAAGTTTAGTGGATGGGATCAGCCTGTTCGGTTTTCAATCA / CGCTCTAGAGCGGCTCGGCGGGGTTTT	
arsH1-1f/1r (380 bp)	CGCGGATCCAACCGGCCTTTCGTCGTCACACC / CCCATCCACTAAACTTAAACACGGGAGCCTCGTCGGGAAGC	For deletion of *arsH1* gene and for RT-PCR of *arsC2-arsH1*
arsH1-2f/2r (233 bp)	TGTTTAAGTTTAGTGGATGGGCGATGGCCGGATGAAAC / CGCTCTAGAGCCCGCGCTCGCAGTGATT	
arsR-2f/ars12RT-r (585 bp)	CTTCGGCGAGGATTGAGC	For RT-PCR of *arsR1-arsC1* and for ArsR1-ParsC1 binding assay
ars23RT-f/r (343 bp)	GGTGAAGCCTGCCCGGTATGGAT / TGAAAAACGCCGGGGATGAAATGG	For RT-PCR of *arsC1-acr3*

incubated at 30°C until colonies formed (1 to 3 days). Alternatively, cultures were grown overnight at 30°C in liquid $MMNH_4$, diluted into same media to an $Ab_{595} = 0.4$ and serially diluted in 10-fold steps. Diluted cell suspensions were then spot inoculated on $MMNH_4$ agar plates containing varying concentrations of SbIII or AsIII and then incubated at 30°C.

RT-PCR analysis of gene expression

Reverse transcription (RT)-PCR was one method used to investigate gene expression, and was performed as previously described (Kashyap *et al*., 2006a,b). Cells were incubated in the same medium with or without 0.1 mM AsIII. Total RNA was extracted at the exponential phase ($OD_{595} \sim 0.4$-0.5) with the RNeasy kit (Qiagen, Valencia, CA, USA) in accordance with the manufacturer's instructions. Deoxyribonucleic acid was removed by DNase I (Ambion, Grand Island, NY, USA) treatment and purified using a Turbo DNA-free kit (Ambion). Purified RNA was verified to be DNA free via PCRs using 16S RNA gene primers and then 50 ng (in each RT reaction) was reverse transcribed into cDNA using the Avian Myeloblastosis Virus reverse transcriptase (Promega, Madison, WI, USA)

with gene-specific primers (Table 1) according to the manufacturer's instructions. Standardized PCRs with the cDNA were conducted at 94°C for 5 min and 30 cycles of 94°C for 30 s, 60°C for 1 min and 68°C for 1 min. The final extension was performed at 68°C for 5 min.

ArsR-1 purification and EMSA

The His-tagged ArsR-1 protein was purified as described previously (Kang *et al*., 2012a). Regions of DNA representing different segments of the putative *ars1* operon (*arsR-1* to *acr3-1*; Fig. 1) were examined for ArsR-1 binding targets using specific segments of DNA PCR amplified from the 5A wild-type strain. After amplification, the DNA fragments were purified using QIAquick PCR purification kit (Qiagen), with 35 nM of DNA mixed with ArsR1-His6 (0 or 0.8 μM) in binding buffer (100 mM HEPES, pH 7.5, 0.5 mM potassium chloride, 5 mM dithiothreitol and 25% glycerol) with or without 1 mM AsIII in a total volume of 15 μl and incubated at RT for 45 min. The reaction mixtures were then electrophoresed through 6% native polyacrylamide gels using Tris-borate buffer (90 mM Tris, 90 mM boric acid and 0.02 M EDTA, pH 8.0) at 100 V for 2 h at room temperature. Gels were stained with ethidium bromide (5 μg ml^{-1}) for 30 min and rinsed with distilled water and visualized by UV.

aioB reporter assays

The *aioB* promoter region-lacZ fusion vector, pLSP-P*aioB*, was used for the analysis of P*aioB* promoter activity responding to AsIII treatment in the wild-type, Δ*acr3-1*, Δ*acr3-2* and Δ*dctA* mutant cells. The standard induction media was 20 ml of MMN with 50 μM Pi and 100 μM AsIII. For some assays, additional AsIII (up to 3 mM) was added to cultures growing in the standard medium. Cultures were incubated at 30°C on a rotary shaker. After the various incubation times, β-galactosidase assays were conducted as we have previously described (Kang *et al*., 2012a,b).

Acr3 phylogenetic analysis

Phylogenetic analysis of Acr3-1 and Acr3-2-inferred amino acid sequences was performed using MEGA version 5.2.2 software (http://www.megasoftware.net/mega.php; Tamura *et al*., 2011), using the Maximum Likelihood algorithm. Bootstrap values for the tree branch points were calculated from 100 pseudoreplicates.

Acknowledgements

The authors thank B.P. Rosen for helpful discussion regarding the EMSA data. This research was primarily supported by the U.S. National Science Foundation to T.R.M and B.B. (MCB 0817170), and by the Montana Agricultural Experiment Station (911310) to T.R.M. Z.S. was supported by a PhD student exchange scholarship of the Ministry of Education, P. R. of China as part of a Major International Joint Research Project of Chinese National Natural Science Foundation (31010103903) to G.W. (Co-PI T.R.M.).

References

Aaltonen, E.K., and Silow, M. (2008) Transmembrane topology of the Acr3 family arsenite transporter from *Bacillus subtilis*. *Biochim Biophys Acta* **1778:** 963–973.

Achour, A.R., Bauda, P., and Billard, P. (2007) Diversity of arsenite transporter genes from arsenic-resistant soil bacteria. *Res Microbiol* **158:** 128–137.

Ajees, A.A., Yang, J., and Rosen, B.P. (2011) The ArsD As(III) metallochaperone. *Biometals* **24:** 391–399.

Anderson, G.L., Williams, J., and Hille, R. (1992) The purification and characterization of arsenite oxidase from *Alcaligenes faecalis*, a molybdenum-containing hydroxylase. *J Biol Chem* **267:** 23674–23682.

Arsène-Ploetze, F., Koechler, S., Marchal, M., Coppée, J.Y., Chandler, M., Bonnefoy, V., *et al*. (2010) Structure, function, and evolution of the *Thiomonas* spp. genome. *PLoS Genet* **6:** e1000859.

Boyer, H.W., and Roulland-Dussoix, D. (1969) A complementation analysis of the restriction and modification of DNA in Escherichia coli. *J Mol Biol* **41:** 459–472.

Branco, R., Chung, A.P., and Morais, P.V. (2008) Sequencing and expression of two arsenic resistance operons with different functions in the highly arsenic-resistant strain *Ochrobactrum tritici* SCII24T. *BMC Microbiol* **8:** 95. 13.

Butcher, B.G., Deane, S.M., and Rawlings, D.E. (2000) The chromosomal arsenic resistance genes of *Thiobacillus ferrooxidans* have an unusual arrangement and confer increased arsenic and antimony resistance to *Escherichia coli*. *Appl Environ Microbiol* **66:** 1826–1833.

Cai, L., Liu, G., Rensing, C., and Wang, G. (2009) Genes involved in arsenic transformation and resistance associated with different levels of arsenic-contaminated soils. *BMC Microbiol* **9:** 4. 8.

Chen, C., Misra, T.K., Silver, S., and Rosen, B.P. (1986) Nucleotide sequence of the structural genes for an anion pump: the plasmid-encoded arsenical resistance operon. *J Biol Chem* **261:** 15030–15038.

Chen, Y., and Rosen, B.P. (1997) Metalloregulatory properties of the ArsD repressor. *J Biol Chem* **272:** 14257–14262.

Cuebas, M., Villafanem, A., McBridem, M., Yeem, N., and Bini, E. (2011) Arsenate reduction and expression of multiple chromosomal *ars* operons in *Geobacillus kaustophilus* A1. *Microbiology* **157:** 2004–2011.

Cullen, W.R., and Reimer, K.J. (1989) Arsenic speciation in the environment. *Chem Rev* **89:** 713–764.

Dey, S., and Rosen, B.P. (1995) Dual mode of energy coupling by the oxyanion-translocating ArsB protein. *J Bacteriol* **177:** 385–389.

Dey, S., Dou, D., Tisa, L.S., and Rosen, B.P. (1994) Interaction of the catalytic and membrane subunits of an oxyanion-translocating ATPase. *Arch Biochem Biophys* **311:** 418–424.

Diorio, C., Cai, J., Marmor, J., Shinder, R., and DuBow, M.S. (1995) An *Escherichia coli* chromosomal *ars* operon homolog is functional in arsenic detoxification and is conserved in gram-negative bacteria. *J Bacteriol* **177:** 2050–2056.

Ditta, G., Stanfield, S., Corbin, D., and Helinski, D.R. (1980) Broad host range DNA cloning system for gram-negative bacteria: construction of a gene bank of Rhizobium meliloti. *Proc Natl Acad Sci USA* **77:** 7347–7351.

Duquesne, K., Lieutaud, A., Rotouchniak, J., Muller, D., Lett, M.C., and Bonnefoy, V. (2008) Arsenite oxidation by a chemoautotrophic moderately acidophilic *Thiomonas* sp.: from the strain isolation to the gene study. *Environ Microbiol* **10:** 228–237.

Fu, H.L., Meng, Y., Ordóñez, E., Villadangos, A.F., Bhattacharjee, H., Gil, J.A., *et al*. (2009) Properties of arsenite efflux permeases (Acr3) from *Alkaliphilus metalliredigens* and *Corynebacterium glutamicum*. *J Biol Chem* **284:** 19887–19895.

Furbank, R.T., Agostino, A., and Hatch, M.D. (1990) C4 acid decarboxylation and photosynthesis in bundle sheath ceils of NAD-malic enzyme-type C4 plants: mechanism and the role of malate and orthophosphate. *Arch Biochem Biophys* **276:** 374–381.

Ghosh, M., Shen, J., and Rosen, B.P. (1999) Pathways of As(III) detoxification in *Saccharomyces cerevisiae*. *Proc Natl Acad Sci USA* **96:** 5001–5006.

vanden Hoven, R.N., and Santini, J.M. (2004) Arsenite oxidation by the heterotroph *Hydrogenophaga* sp. str. NT-14: the arsenite oxidase and its physiological electron acceptor. *Biochim Biophys Acta* **1656:** 148–155.

Indriolo, E., Na, G., Ellis, D., Salt, D.E., and Banks, J.A. (2010) A vacuolar arsenite transporter necessary for arsenic tolerance in the arsenic hyperaccumulating fern *Pteris vittata* is missing in flowering plants. *Plant Cell* **22:** 2045–2057.

Inskeep, W.P., McDermott, T.R., and Fendorf, S.E. (2001) Arsenic (V)/(III) cycling in soils and natural waters: chemical and microbiological processes. In *Environmental Chemistry of Arsenic*. Frankenberger, W.F., Jr, and Macy, J.M. (eds). New York, USA: Marcell Dekker, pp. 183–215.

Ji, G., and Silver, S. (1992a) Regulation and expression of the arsenic resistance operon from *Staphylococcus aureus* plasmid pI258. *J Bacteriol* **174:** 3684–3694.

Ji, G., and Silver, S. (1992b) Reduction of arsenate to arsenite by the ArsC protein of the arsenic resistance operon of *Staphylococcus aureus* plasmid pI258. *Proc Natl Acad Sci USA* **89:** 7974–7978.

Kang, Y.S., and Park, W. (2010) Trade-off between antibiotic resistance and biological fitness in *Acinetobacter* sp. Strain DR1. *Environ Microbiol* **12:** 1304–1318.

Kang, Y.S., Heinemann, J., Bothner, B., Rensing, C., and McDermott, T.R. (2012a) Integrated co-regulation of bacterial arsenic and phosphorus metabolisms. *Environ Microbiol* **14:** 3097–3109.

Kang, Y.S., Bothner, B., Rensing, C., and McDermott, T.R. (2012b) Involvement of RpoN in regulating bacterial arsenite oxidation. *Appl Environ Microbiol* **78:** 5638–5645.

Kaplan, R.S., and Pedersen, P.L. (1985) Isolation and reconstitution of the n-butylmalonate-sensitive dicarboxylate transporter from rat liver mitochondria. *J Biol Chem* **260:** 10293–10298.

Kashyap, D.R., Botero, L.M., Franck, W.L., Hassett, D.J., and McDermott, T.R. (2006a) Complex regulation of arsenite oxidation in *Agrobacterium tumefaciens*. *J Bacteriol* **188:** 1081–1088.

Kashyap, D.R., Botero, L.M., Lehr, C., Hassett, D.J., and McDermott, T.R. (2006b) A Na^+:H^+ antiporter and molybdate transporter are essential for arsenite oxidation in *Agrobacterium tumefaciens*. *J Bacteriol* **188:** 1577–1584.

Koechler, S., Cleiss-Arnold, J., Proux, C., Sismeiro, O., Dillies, M.A., Goulhen-Chollet, F., *et al*. (2010) Multiple controls affect arsenite oxidase gene expression in *Herminiimonas arsenicoxydans*. *BMC Microbiol* **10:** 53–65.

Lebrun, E., Brugna, M., Baymann, F., Muller, D., Lievremont, D., Lett, M.C., and Nitschke, W. (2003) Arsenite oxidase, an ancient bioenergetic enzyme. *Mol Biol Evol* **20:** 686–693.

Li, B., Lin, J., Mi, S., and Lin, J. (2010) Arsenic resistance operon structure in *Leptospirillum ferriphilum* and proteomic response to arsenic stress. *Bioresour Technol* **101:** 9811–9814.

Lieutaud, A., van Lis, R., Duval, S., Capowiez, L., Muller, D., Lebrun, R., *et al*. (2010) Arsenite oxidase from *Ralstonia* sp. 22: characterization of the enzyme and its interaction with soluble cytochromes. *J Biol Chem* **285:** 20433–20441.

Lin, Y.F., Walmsley, A.R., and Rosen, B.P. (2006) An arsenic metallo-chaperone for an arsenic detoxification pump. *Proc Natl Acad Sci USA* **103:** 15617–15622.

Liu, G., Liu, M., Kim, E.H., Matty, W., Bothner, B., Lei, B., *et al*. (2012) A periplasmic arsenite-binding protein involved in regulating arsenite oxidation. *Environ Microbiol* **12:** 1624–1634.

Lopez-Maury, L., Florencio, F.J., and Reyes, J.C. (2003) Arsenic sensing and resistance system in the cyanobacterium *Synechocystis* sp. strain PCC 6803. *J Bacteriol* **185:** 5363–5371.

Maciaszczyk-Dziubinska, E., Wawrzycka, D., Slama, E., Migocka, M., and Wysocki, R. (2010) The yeast permease Acr3p is a dual arsenite and antimonite plasma membrane transporter. *Biochim Biophys Acta* **1798:** 2170–2175.

Mukhopadhayay, R., Rosen, B.P., Phung, L.T., and Silver, S. (2002) Microbial arsenic: from geocycles to genes and enzymes. *FEMS Microbiol Rev* **26:** 311–325.

Muller, D., Lièvremont, D., Simeonova, D.D., Hubert, J.C., and Lett, M.C. (2003) Arsenite oxidase aox genes from a metal-resistant beta-proteobacterium. *J Bacteriol* **185:** 135–141.

Murphy, J.N., and Saltikov, C.W. (2009) The ArsR repressor mediates arsenite-dependent regulation of arsenate respiration and detoxification operons of *Shewanella* sp. strain ANA-3. *J Bacteriol* **191:** 6722–6731.

Ordóñez, E., Letek, M., Valbuena, N., Gil, J.A., and Mateos, L.M. (2005) Analysis of genes involved in arsenic resistance in *Corynebacterium glutamicum* ATCC 13032. *Appl Environ Microbiol* **71:** 6206–6215.

Oremland, R.S., and Stolz, J.F. (2003) The ecology of arsenic. *Science* **300:** 939–944.

Pontius, F.W., Brown, K.G., and Chen, C.-J. (1994) Health implications of arsenic in drinking water. *J AWWA* **86:** 52–63.

Prasad, K.S., Subramanian, V., and Paul, J. (2009) Purification and characterization of arsenite oxidase from *Arthrobacter* sp. *Biometals* **22:** 711–721.

Rosen, B.P. (1999) Families of arsenic transporters. *Trends Microbiol* **7:** 207–212.

Rosen, B.P. (2002) Biochemistry of arsenic detoxification. *FEBS Lett* **529:** 86–92.

Rosen, B.P., Dey, S., Dou, D., Ji, G., Kaur, P., Ksenzenko, M.Y., *et al*. (1992) Evolution of an ion-translocating ATPase. *Ann N Y Acad Sci* **671:** 257–272.

Rosenstein, R., Peschel, A., Wieland, B., and Gotz, F. (1992) Expression and regulation of the antimonite, arsenite, and arsenate resistance operon of *Staphylococcus xylosus* plasmid pSX267. *J Bacteriol* **174:** 3676–3683.

Ryan, D., and Colleran, E. (2002) Arsenical resistance in the IncHI2 plasmids. *Plasmid* **47:** 234–240. 2002 May.

San Francisco, M.J.D., Hope. C.L., Owolabi, J.B., Tisa, L.S., and Rosen, B.P. (1990) Identification of the metalloregulatory element of the plasmid-encoded arsenical resistance operon. *Nucleic Acids Res* **18:** 619–624.

Santini, J.M., Lindsay, I.S., Schnagl, R.D., and Macy, J.M. (2000) A new chemolithoautotrophic arsenite-oxidizing bacterium isolated from a gold mine: phylogenetic, physiological, and preliminary biochemical studies. *Appl Environ Microbiol* **66:** 92–97.

Sardiwal, S., Santini, J.M., Osborne, T.H., and Djordjevic, S. (2010) Characterization of a two-component signal transduction system that controls arsenite oxidation in the chemolithoautotroph NT-26. *FEMS Microbiol Lett* **313:** 20–28.

Sato, T., and Kobayashi, Y. (1998) The *ars* operon in the skin element of *Bacillus subtilis* confers resistance to arsenate and arsenite. *J Bacteriol* **180:** 1655–1661.

Silver, S., Ji, G., Bröer, S., Dey, S., Dou, D., and Rosen, B.P. (1993) Orphan enzyme or patriarch of a new tribe: the arsenic resistance ATPase of bacterial plasmids. *Mol Microbiol* **8:** 637–642.

Silver, S., Phung, L.T., and Rosen, B.P. (2001) Arsenic metabolism: resistance, reduction, and oxidation. In *Environmental Chemistry of Arsenic*. Frankenberger, W.F., Jr, and Macy, J.M. (eds). New York, USA: Marcell Dekker, pp. 247–272.

Somerville, J.E., and Kahn, M.L. (1983) Cloning of the glutamine synthetase I gene from *Rhizobium meliloti*. *J Bacteriol* **156:** 68–176.

Stock, J.B., Surette, M.G., Levit, M., and Park, P. (1995) Two-component signal transduction systems: structure-function relationships and mechanisms of catalysis. In *Two-Component Transduction*. Hoch, J.A., and Silhavy, T.J. (eds). Washington D.C., USA: ASM Press, pp. 25–51.

Stolz, J.F., Basu, P., Santini, J.M., and Oremland, R.S. (2006) Arsenic and selenium in microbial metabolism. *Annu Rev Microbiol* **60:** 107–130.

Tamura, K., Peterson, D., Peterson, N., Stecher, G., Nei, M., and Kumar, S. (2011) MEGA5: molecular evolutionary genetics analysis using maximum likelihood, evolutionary distance, and maximum parsimony methods. *Mol Biol Evol* **28:** 2731–2739.

Tisa, L.S., and Rosen, B.P. (1989) Molecular characterization of an anion pump: the ArsB protein is the membrane anchor for the ArsA protein. *J Biol Chem* **265:** 190–194.

Wu, J., and Rosen, B.P. (1993) The *arsD* gene encodes a second trans-acting regulatory protein of the plasmid-encoded arsenical resistance operon. *Mol Microbiol* **8:** 615–623.

Wysocki, R., Bobrowicz, P., and Ulaszewski, S. (1997) The *Saccharomyces cerevisiae* ACR3 gene encodes a putative membrane protein involved in arsenite transport. *J Biol Chem* **272:** 30061–30066.

Xia, X., Postis, V.L., Rahman, M., Wright, G.S., Roach, P.C., Deacon, S.E., *et al*. (2008) Investigation of the structure and function of a *Shewanella oneidensis* arsenical-resistance family transporter. *Mol Membr Biol* **25:** 691–705.

Yang, H.C., Cheng, J., Finan, T.M., Rosen, B.P., and Bhattacharjee, H. (2005) Novel pathway for arsenic detoxification in the legume symbiont *Sinorhizobium meliloti*. *J Bacteriol* **187:** 6991–6997.

Ye, J., Yang, H.-C., Rosen, B.P., and Bhattacharjee, H. (2007) Crystal structure of the flavoprotein ArsH from *Sinorhizobium meliloti*. *FEBS Lett* **581:** 3996–4000.

Zargar, K., Hoeft, S., Oremland, R.S., and Saltikov, C. (2010) Identification of a novel arsenite oxidase gene, *arxA*, in the haloalkaliphilic, arsenite-oxidizing bacterium *Alkalilimnicola ehrlichii* strain MLHE-1. *J Bacteriol* **192:** 3755–3762.

Zargar, K., Conrad, A., Bernick, D.L., Lowe, T.M., Stolc, V., Hoeft, S., *et al*. (2012) ArxA, a new clade of arsenite oxidase within the DMSO reductase family of molybdenum oxidoreductases. *Environ Microbiol* **14:** 1635–1645.

Supporting information

Additional Supporting Information may be found in the online version of this article at the publisher's web-site:

Fig. S1. Example RT-PCR illustrating polar effect on expression of genes downstream of *arsR1::tetRA*. RT-PCR was performed with *arsR-1-arsC-1* specific primers (Table 1) that amplifies downstream of the tetRA insertion in the *arsR-1* coding region and includes the 5′ region of *arsC-1*. Total RNA was extracted at the early exponential phase from wild-type or *arsR1::tetRA* mutant cells grown in MMN medium with or without 0.1 mM AsIII. Molecular weight markers are shown in far left lane.

Fig. S2. The Δ*acr3-2* mutant is positive for AsIII oxidation, regardless of the agar AsIII concentration. The wild-type strain 5A and the Δ*acr3-2* mutant were streaked onto $MMNH_4$ agar containing 100 mM Pi and 1.0 mM, 2.0 mM or 3.0 mM AsIII, incubated at 30°C and then stained for AsIII oxidation activity using silver nitrate as a qualitative stain for detecting AsV (brown precipitate). See Materials and Methods in the manuscript for details.

Fig. S3. RT-PCR analysis illustrating the co-transcription of the *ars1* locus genes and their enhanced and constitutive expression in the *ΔarsR-1* mutant, with or without AsIII. RT-PCRs were performed with *ars1* region specific primers (Table 1) that prime from within the: (i) 3′ coding region of *arsR-1* and the 5′ coding region of *arsC-1*; (ii) the 3′ coding

region of *arsC-1* and the 5′ coding region of *acr3-1*; (iii) 3′ coding region *arsC-2* to the 5′ coding region of *arsH*; and (iv) 3′ region of *arsR1* to the 5′ region of *acr3-1*. Total RNA was extracted at the early exponential phase from wild-type or *ΔarsR-1* mutant cells grown in $MMNH_4$ medium with or without 0.1 mM AsIII. Molecular weight markers are shown in far left lane. All reverse transcriptase reactions contained 15 ng of RNA, and each lane was loaded with 10 μl of the PCR product except for the 16S rRNA gene, where 6 μl were used.

Fig. S4. Acr3-2 supplements trivalent metalloid resistance at higher AsIII and SbIII concentrations. Growth of the wild-type, Δ*acr3-1* and Δ*acr3-2* mutants on $MMNH_4$ agar medium containing 3.0 mM AsIII or 0.06 mM SbIII. Each culture was first normalized to O.D. ~ 0.4, and then serially diluted 10-fold, with each dilution spotted onto the agar medium (10 μl each), and then incubated at 30°C for 24 h. Note that the Δacr3-2 mutant exhibited WT level growth on 1 mM or 2 mM AsIII, and on 0.02 mM SbIII.

Fig. S5. Characterization of *A. tumefaciens* strain 5A Acr3 anti-porters. (A) Phylogenetic relatedness as estimated using the maximum-likelihood algorithm in MEGA. Bootstrap values > 50% based on 100 replicates are given at branch points. Bar, 0.2 substitutions per amino acid position. (B) Structure predictions for Acr3-1 and Acr3-2. Image was generated using the PredictProtein software (http://www.predictprotein.org). Predicted structural elements are shown relative to the amino acid number positions scale at top. Secondary structure code: brown boxes designate predicted helix-type structures and blue predicts strand-type. Solvent accessibility code: yellow indicates buried and blue indicates exposed.

Fig. S6. Characterization of the wild-type strain 5A and the Δ*acr3-2* and Δ*dctA* mutants for growth (A) and regulation of *aioB* (B) in response to elevated concentrations of AsIII. For each culture, cells were inoculated into $MMNH_4$ media containing 50 μM phosphate and 100 μM AsIII, incubated for 5 h, at which time additional AsIII was added (arrow) to increase the AsIII concentration to 3 mM. Data are the means from duplicate cultures, and where visible the error bars represent ± 1 SD.